

Interlayer Reactions of the Silver Molybdate $\text{Ag}_6\text{Mo}_{10}\text{O}_{33}$

CHRISTIAN RÖSNER AND GERHARD LAGALY

*Institut für Anorganische Chemie der Universität Kiel,
Olshausenstrasse 40, D-2300 Kiel, Germany*

Received October 12, 1983; in revised form December 30, 1983

Silver molybdate $\text{Ag}_6\text{Mo}_{10}\text{O}_{33}$ exchanges silver ions for organic cations, particularly surface-active agents such as long-chain *n*-alkylammonium ions $\text{C}_n\text{H}_{2n+1}\text{NH}_3^+$. The alkylammonium ions penetrate between the layers and aggregate as bimolecular structures. The alkyl chains in the interlayer are not in all-*trans* conformation but are isomerized into conformers with *gauche*-bonds. These chains aggregate as *gauche*-blocks because the polar chain ends (NH_3^+ and NH_2 groups) interacting with the molybdate layer cannot be close-packed. The specially favored formation and pronounced stability of *gauche*-blocks impede the quantitative exchange of the silver ions. No more than 20% of the silver ions are exchanged by alkylammonium nitrate. The *gauche*-blocks are stabilized by additional uptake of alkylamine molecules. Silver molybdate also reacts with alkylamine and forms long-spacing complexes with long segments of the alkyl chains perpendicular to the layers.

Introduction

Many polyacid salts $\text{A}_x\text{M}_y\text{O}_z$ of IV, V, and VI-group transition elements form layered host compounds with distinct intracrystalline reactivity (1, 8, 9). The exchange of organic cations for the inorganic interlayer cations is particularly pronounced. Inorganic cations displace only small amounts of interlayer cations.

Surprisingly, long-chain organic cations are most reactive. The reactivity of the long-chain cations becomes plausible if one considers their surface activity. The cations have a strong tendency to aggregate as monomolecular films on solid and liquid surfaces. The long-chain cations penetrate between the interlamellar surfaces of the layered host compounds and aggregate in distinct structures. The type of aggregation of long-chain compounds on interlamellar

surfaces (7) is more multifarious than initially expected. The interlayer alkyl chain orientation cannot be understood without considering conformational changes of the alkyl chains. The basic principles of such changes are well known from studies in polymer, interface and colloid chemistry, and particularly biophysics (biomembrane studies). Among the molybdates listed by Beneke and Lagaly (1), the silver molybdate $\text{Ag}_6\text{Mo}_{10}\text{O}_{33}$ is of particular interest because only a part of the silver ions is displaced by alkylammonium ions; this is directly related to the type of interlamellar chain aggregation.

Materials and Methods

$\text{Ag}_6\text{Mo}_{10}\text{O}_{33}$. The silver molybdate can best be prepared from melts of Ag_2MoO_4 and MoO_3 in the ratio 1 : 2. The ratio should

be slightly above 3:7 (the ratio in $\text{Ag}_6\text{Mo}_{10}\text{O}_{33}$) to obtain uniform crystals. This is in agreement with the phase diagram (5) which exhibits a peritectic point at 35 mole% Ag_2MoO_4 . Gatehouse and Leverett (2, 4) also started from melts of $\text{Ag}_2\text{MoO}_4 + 2\text{MoO}_3$ to prepare single crystals. Consequently, the composition of the silver molybdate was first reported as being $\text{Ag}_2\text{Mo}_3\text{O}_{10}$ ($\hat{=}$ $\text{Ag}_2\text{MoO}_4 : \text{MoO}_3 = 1 : 2$). However, the correct and rather unexpected formula $\text{Ag}_6\text{Mo}_{10}\text{O}_{33}$ for this compound has been determined through a complete crystal structure analysis (3, 4).

Thus, larger amounts of silver molybdate were prepared by melting 1 mole of Ag_2MoO_4 and 2 moles of MoO_3 in a porcelain crucible at 650–700°C for 18 hr, similar to the procedure of Gatehouse and Leverett (2). After slow cooling down, needle-shaped, yellow-colored crystals of silver molybdate were obtained which could easily be separated from some of the remaining compact material. Microscopic inspection revealed a very uniform material without any detectable impurities. For most investigations the crystals were ground in a mortar to a fine powder with light yellow color.

Ag_2MoO_4 was obtained following the procedure of Ricci and Linke (12). Thus, 200 ml of 1 M AgNO_3 and 100 ml of 1 M $\text{Na}_2\text{MoO}_4 \cdot 2\text{H}_2\text{O}$ were added dropwise to 1 liter of boiling water. The precipitate was washed free of sodium ions with water, first dried at room temperature *in vacuo*, and then for 1 hr at 65°C *in vacuo* <10 Pa.

The powder diagram of $\text{Ag}_6\text{Mo}_{10}\text{O}_{33}$ was identical with that reported by Kohlmüller and Faurie (5).

Organic long-chain compounds. Long-chain primary *n*-alkylamines and the corresponding ammonium salts as surface active agents are best suited for intracrystalline reactions. The alkylamines $\text{C}_n\text{H}_{2n+1}\text{NH}_2$ ($n = 1, 2, \dots, 18$) were used as received (Fluka AG, Switzerland). Solutions of the corresponding chlorides and nitrates were pre-

pared by adding equivalent amounts of HCl or HNO_3 to solutions of the alkylamines in water/ethanol (9:1) and adjusting the pH to about 6. (Concentrations: 2 M for $n = 3-6$, 0.5 M for $n = 7-9$, 0.1 M for $n = 10-14$, and 0.05 M for $n = 15-18$.)

Intracrystalline reactions. About 100 mg of finely powdered silver molybdate were reacted with 5 ml 0.1 M alkylammonium nitrate solutions ($n = 10-15$) in test tubes enclosed by plastic caps. For $n < 10$, 1–2 ml of 0.5 M solution and, for $n > 15$, 10 ml of 0.05 M solution were used. Samples with $n < 10$ were reacted for 2 weeks, with $n \geq 10$ five days at 65°C under occasional shaking. The solid was then separated by centrifugation and X-rayed while in contact with the mother liquid. To remove the excess of alkylammonium salt, the samples were washed 6 times with 7 ml ethanol/water (1:1), finally with 7 ml ethanol, dried first in air and then for 1 hr at 65°C *in vacuo* (<10 Pa). X-Ray powder diagrams were taken from the air-dried and from the vacuum-dried materials.

Very pure alkylammonium derivatives were obtained by using solutions of alkylammonium chlorides. The silver chloride was removed by a short wash with a 15% solution of thiourea in water/acetone (1:1), followed by more intense washing with ethanol/water.

Silver molybdate was also directly reacted with alkylamines. The powdered molybdate was brought into contact with the liquid alkylamines for at least 2 days. Solid alkylamines were mixed with silver molybdate. The mixtures were allowed to stand 2 days at 65°C. In both cases the suspensions were transferred into Lindemann glass tubes and X-rayed.

By reacting with alkylammonium ions or alkylamines, the crystals of silver molybdate were broken into very fine fragments. Only X-ray powder diagrams could be obtained.

All X-ray measurements were made in

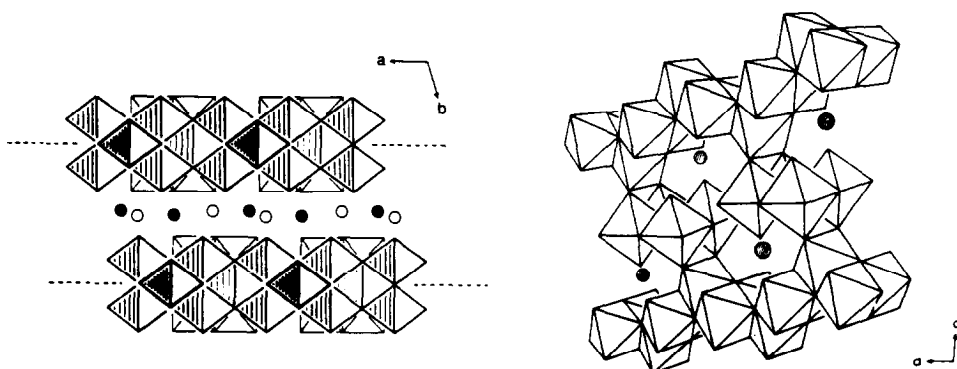


FIG. 1. The layer structure of silver molybdate.

Debye-Scherrer powder cameras with increased diameter (114.59 mm) and $\text{CuK}\alpha$ -radiation.

The intracrystalline reactions increase the spacing between the molybdate layers and thus, the b_0 -dimension. In case of small lattice expansions, the interpretation of the powder diagram can be complicated. The intracrystalline reaction with long-chain compounds results in large lattice expansions. The powder diagram then shows a distinct, well-developed series of sharp reflections following a very intense reflection at high d -value (15–60 Å). The corresponding $1/d$ -values are multiples of the $1/d$ -value of the first, very intense reflection; this allows the reflections to be easily identified. As usual (10, 14) these reflections are taken as basal reflections d_{0k0} . The basal spacing is $d_L = kd_{0k0}$. The strongly increased intensity of the first-order reflections is caused by the weak diffraction power of the organic interlayers as compared with that of the layers (cf. Weiss *et al.* (13) and Lagaly (8, 9)).

Analytical determinations. For potentiometric Ag and Mo-determinations, the samples were dissolved in 20 ml of concentrated sulfuric acid under moderate heating. The solutions were diluted with water to 250 ml.

Silver was determined by potentiometric

titration with sodium chloride. Molybdenum was reduced to Mo(III) using a Jones reductor with cadmium amalgam, then potentiometrically titrated with cerium(IV) sulfate. Carbon was obtained by combustion.

The degree of cation exchange with alkylammonium ions was derived from 1, the amount of silver liberated to the solution and 2, the silver content of the exchanged samples (after washing and in vacuum-drying).

Results

Analytical Composition

From $\text{Ag}_2\text{MoO}_4/\text{MoO}_3$ melts two silver molybdates can be obtained: $\text{Ag}_2\text{Mo}_2\text{O}_7$ and $\text{Ag}_6\text{Mo}_{10}\text{O}_{33}$. The latter crystallizes over quite a wide range of composition in the phase system; the actual composition of the crystals often deviates from the ideal stoichiometry $\text{Ag}_6\text{Mo}_{10}\text{O}_{33}$. The sample used for the cation exchange experiments had a Ag/Mo ratio of 6.49/10.

The increased silver content was noted earlier (4) and was explained as arising through admixtures of $\text{Ag}_2\text{Mo}_2\text{O}_7$.

As mentioned above, impurities in our products could not be detected by microscopic inspection. The reaction with alkylammonium ions provides a sensitive

TABLE I
ANALYTICAL COMPOSITION OF ALKYLAMMONIUM-EXCHANGED SILVER MOLYBDATES
(WASHED, VACUUM-DRIED)

n	moles/100 g			moles/10 moles Mo			
	Mo	Ag	$\text{RNH}_2, \text{RNH}_3^+$	Ag	$\text{RNH}_2, \text{RNH}_3^+$	RNH_3^+	RNH_2
0	0.465	0.302	—	6.49	—	—	—
3	0.454	0.308	1.94×10^{-3}	6.78	0.04	—	(0.04)
4	0.423	0.306	3.51×10^{-3}	7.23	0.08	—	(0.08)
5	0.455	0.298	1.20×10^{-2}	6.55	0.26	—	(0.26)
6	0.456	0.290	2.72×10^{-2}	6.36	0.60	0.13	0.47
7	0.412	0.282	4.26×10^{-2}	6.84	1.03	—	(1.03)
8	0.435	0.270	5.62×10^{-2}	6.21	1.29	0.28	1.01
9	0.421	0.260	5.16×10^{-2}	6.18	1.23	0.31	0.92
10	0.407	0.242	6.38×10^{-2}	5.95	1.57	0.54	1.03
11	0.413	0.236	6.94×10^{-2}	5.71	1.68	0.78	0.90
12	0.398	0.224	7.10×10^{-2}	5.63	1.78	0.86	0.92
13	0.402	0.238	7.42×10^{-2}	5.92	1.85	0.57	1.28
14	0.330	0.212	7.40×10^{-2}	6.42	2.24	0.07	2.17
	0.290	0.163	6.38×10^{-2}	5.55	2.20	0.87	1.33
15	0.282	0.152	8.78×10^{-2}	5.39	3.11	1.10	2.11
18	0.280	0.152	1.18×10^{-1}	5.43	4.21	1.06	3.15

Note. Alkylammonium ion = $\text{C}_n\text{H}_{2n+1}\text{NH}_3^+$.

method for detecting admixed materials (13), even if both compounds are very similar such as smectites in clays (cf. Lagaly (9)). However, no material other than $\text{Ag}_6\text{Mo}_{10}\text{O}_{33}$ could be detected by alkylammonium ion exchange. $\text{Ag}_2\text{Mo}_2\text{O}_7$ or Ag_2MoO_4 would easily be recognized by their different basal spacings after the alkylammonium ion exchange. Thus, we had to reject the assumption that the silver molybdate contains $\text{Ag}_2\text{Mo}_2\text{O}_7$ or Ag_2MoO_4 .

An increased Ag/Mo ratio might result from the presence of molybdenum ions of lower valency. The analytical determinations exhibited no detectable amounts of Mo (<VI), probably because they are oxidized by Ag^+ under formation of Ag^0 . Our actual assumption is that the additional silver is present as Ag^0 , perhaps associated with Ag^+ -ions on the surface or even in the structure. There is a further indication of this mechanism. After reaction with short-chain alkylammonium ions (Table I, Fig. 2)

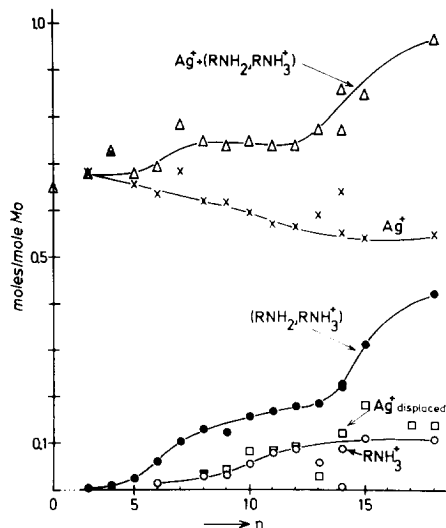


FIG. 2. Analytical composition of alkylammonium-exchanged silver molybdates (washed, vacuum-dried) as a function of alkyl chain length (Ag^+ , displaced: moles of Ag^+ measured in the equilibrium solution. All other values refer to the interlayer composition of the washed and vacuum-dried samples).

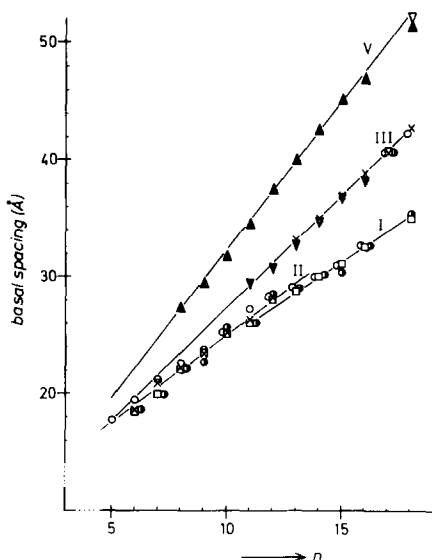


FIG. 3. Basal spacings of alkylamine and alkylammonium-exchanged silver molybdates as a function of alkyl chain length n . Alkylammonium-exchanged silver molybdates: \times , in equilibrium solution; \circ , washed (5 \times), air-dried; \bullet , washed (7 \times), air-dried; \square , washed, air-dried, then vacuum-dried at 65°C. Alkylamine silver molybdate: \blacktriangle , in equilibrium with alkylamine; \blacktriangledown , washed (6 \times), air-dried, vacuum-dried at 65°C.

the Ag/Mo-ratio of the exchanged products can be further increased. In this case some molybdenum ions are reduced during the reaction with alkylammonium ions but are reoxidized by Ag^+ under formation of Ag^0 .

Cation Exchange with Alkylammonium Ions

The analytical composition of the alkylammonium exchanged silver molybdates is listed in Table I. The starting material was a powdered sample of uniform crystals with the stoichiometry $\text{Ag}_{6.49}\text{Mo}_{10}\text{O}_{33}$. The content of $(\text{RNH}_3^+, \text{RNH}_2)$ was calculated from the carbon content, on neglect of the small difference in molecular mass between RNH_3^+ and RNH_2 .

For shorter chain alkyl chains ($n \leq 5$) the Ag/Mo-ratio is 0.65 or even higher (Fig. 2), probably due to the redox process men-

tioned above. For longer chains the ratio decreases with chain length. The $(\text{RNH}_3^+, \text{RNH}_2)/\text{Mo}$ ratio increases sigmoidally. The ratio $(\text{Ag} + \text{RNH}_3^+, \text{RNH}_2)/\text{Mo}$ exhibits a plateau at $n = 7-12$. (We could not obtain reliable data for $n = 16$ and 17, probably due to impurities of the amines.)

In some cases ($n = 7, 13, 14$) the exchange of Ag evidently is too low. However, the $(\text{RNH}_2, \text{RNH}_3^+)$ content measured for the same samples shows no irregularities. By repeating the experiments the exchange ratio was either found as expected or else again was too low. This is understandable, considering the special mechanisms of intracrystalline reactions (see below).

Basal Spacings of Alkylammonium-Exchanged Silver Molybdates

In equilibrium with alkylammonium nitrate solutions the basal spacings range from 18.6 Å ($n = 6$) to 42.8 Å ($n = 18$) (Fig. 3; lines II and III). The increase with chain length is linear from $n = 7$ to $n = 12$ and from $n = 13$ to $n = 18$. Washing with water/ethanol (1/1) and drying does not change the spacings for chains $n \leq 12$. The spacings of the longer chain derivatives are decreased (line I). The mean increase of the straight lines is listed in Table II.

TABLE II
MEAN INCREASE OF THE LINEAR BASAL SPACING CHANGES

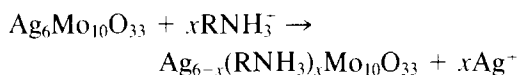
Condition	Alkyl chain length n	Line in Fig. 3	$\Delta d/\Delta n$ (Å)
In equilibrium with alkylammonium ions	7-12	II	1.46
	13-18	III	1.94
Washed and dried	7-12	II	1.46
	13-18	I	1.33
$\text{Ag}_6\text{Mo}_{10}\text{O}_{33}$ + alkylamine then washed, dried	8-15	V	2.54
	11-16	III	1.94

If $\text{Ag}_6\text{Mo}_{10}\text{O}_{33}$ is brought into contact with alkylamines, the amine is directly intercalated. The spacings are on the straight line V, with a mean increase $\Delta d/\Delta n = 2.54 \text{ \AA}$. By washing with ethanol the intercalated alkylamine can only be partly removed from the interlayer space (line III).

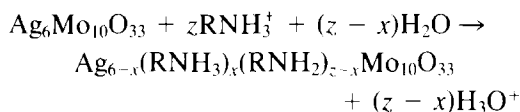
Discussion

Alkylammonium Ion Exchange

Although silver molybdate easily reacts with alkylammonium cations, the degree of exchange is low ($\leq 20\%$). On the other hand, the alkylammonium interlayers are very stable. The stability results from additional intercalation of alkylamine molecules. Thus, the exchange



is accompanied by alkylamine intercalation:



and

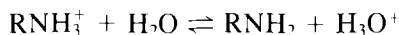


Table I and Fig. 2 show that z increases with chain length from 0.04 for $n = 3$ to 4.2 for $n = 18$. Since z as derived from the carbon content yields the sum $(\text{RNH}_3^+ + \text{RNH}_2)$, a division into RNH_3^+ and RNH_2 contributions was arrived at on the basis of the different silver contents of the silver molybdate and the alkylammonium-exchanged samples. In fact, this number of RNH_3^+ ions agrees with the number of silver ions liberated to the solution (Fig. 2).

The interlayer structure is directed by the alkyl chain density (number of alkyl chains per unit cell). As evidenced by the analytical results, it is not important whether the alkyl chains are placed in the interlayer

space as alkylammonium ions (instead of exchanged silver ions) or as alkylamine molecules. This explains the above-mentioned observations, that samples differing by the degree of exchange show identical basal spacings. The decreased number of alkylammonium ions is counterbalanced by an increased number of alkylamine molecules.

Interlayer Structure

The basal spacings in Fig. 3 indicate three main interlayer structures: a long-spacing structure (line V), a short-spacing structure (lines I, II), and an intermediate form (line III).

Long-Spacing Structure

This structure forms by direct intercalation of alkylamine (line V). The increase of the spacings $\Delta d/\Delta n = 2.54 \text{ \AA}$ at first sight points to bilayers of alkylamine molecules (Figs. 4a and 5a). The spacings should then follow the relation (bond lengths $\text{C-N} \approx \text{C-C}$):

$$d_L = \delta + 2 \times 1.27n + z$$

The nitrogen atoms occupy approximately the positions of the displaced silver ions. The mean distance of the silver ions from interlayer to interlayer is $d_{010} = 7.97 \text{ \AA}$; thus $\delta \approx 8 \text{ \AA}$. The mid-layer distance z of the methyl end groups is approximately 3 \AA . (The exact value depends on the type of methyl end-group packing.) Therefore,

$$d_L = 11 + 2 \times 1.27n (\text{\AA})$$

The experimental data (Fig. 3) follow the relation

$$d_L = 7 + 2 \times 1.27n (\text{\AA})$$

The different of 4 \AA is beyond the uncertainty related to δ and z . The increase of 2.54 \AA definitely indicates that a large section of the chains must be perpendicular to the layers (i.e., to the plane a_0c_0). There are only two possibilities for explaining the de-

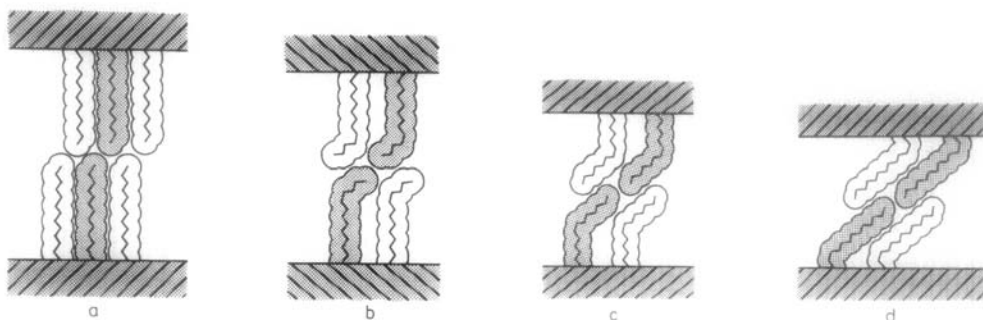


FIG. 4. Bilayer chain aggregation in alkylamine and alkylammonium silver molybdates: (a) bilayers of all-*trans* chains; (b) aggregation of chains with *gauche* conformations near the methyl end groups: long-spacing structures; (c) *gauche*-conformations near the middle of the chains: intermediate structures; (d) *gauche*-conformations very near the polar chain ends = tiled bilayers: short-spacing structures.

creased experimental spacings: either the chains are shortened by kinks or they are aggregated into *gauche*-blocks. In general, shortening by kinks (cf. Figs. 2 and 3 in Ref. (8)) is temperature-dependent and the number of kinks increases with chain length. The insensitivity of the spacings to temperatures up to 120°C and the constant shortening by 4 Å make the existence of *gauche*-block structures more probable. This chain aggregation (Figs. 4b–d) was proposed for certain bilayer arrangements and distinct lipid layers, but then turned out to be a general type of association of chains at lower packing density ($\geq 33 \text{ \AA}^2/\text{chain}$) (7, 8).

The chains in *gauche*-blocks contain iso-

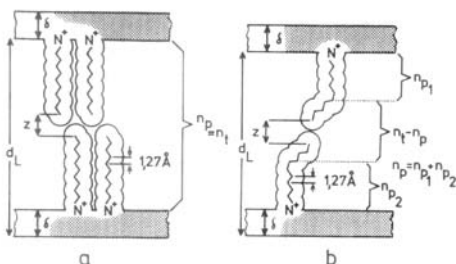


FIG. 5. Calculation of basal spacings (a) blocks of chains in all-*trans* conformation (b) blocks of chains with *gauche*-conformations; n_t : total number of C–C bonds, $n_p = n_{p_1} + n_{p_2}$: number of C–C bonds in the perpendicular segments.

lated *gauche*-bonds or g^+tg^+ -conformations (Pechhold *et al.* (11)). These conformations produce an angle of about 55° in the chain. Such chains can only be close-packed if these conformations are located at different positions in neighboring chains (see Figs. 2 and 3 in Ref. (8)). The *gauche*-conformations can be located at identical positions in neighboring chains (Fig. 4) if the chain ends are held at sufficiently large distances on the solid surface.

The position of the *gauche*-bonds in two adjacent chains determines the layer separation. The “chain pair” (dotted area in Fig. 4) has n_t carbon atoms. The *gauche*-block is described by the maximum number n_p of carbon atoms in the segments perpendicular to the layer.¹ The basal spacing for $n_t, n_p = \text{even}$ or $n_t, n_p = \text{odd}$ (Fig. 5) is

$$d_L = \delta + 1.27n_p + 1.27(n_t - n_p)/2 + z \\ = 11 + 0.63(n_t + n_p)$$

For n_t, n_p even/odd:

$$d_L = \delta + 1.27n_p + 1.27(n_t - n_p - 1)/2 + z \\ d_L = 10.37 + 0.63(n_t + n_p).$$

¹ The n_p represents the highest value within the *gauche*-block and refers to the structure-determining chain pairs (dotted chains in Fig. 4).

TABLE III
LONG-SPACING *Gauche*-BLOCKS OF ALKYLAMINE
BILAYERS IN SILVER MOLYBDATE

<i>n</i>	<i>d_L</i> , obs. (Å)	<i>d_L</i> , calc. (Å)	<i>n_t</i>	<i>n_p</i>	<i>n_t - n_p</i>	<i>n_p/n_t</i>
8	27.4	27.4	16	10	6	0.63
9	29.5	29.9	18	12	6	0.67
10	31.8	32.4	20	14	6	0.70
11	34.6	34.9	22	16	6	0.73
12	37.6	37.5	24	18	6	0.75
13	40.1	40.0	26	20	6	0.77
14	42.7	42.5	28	22	6	0.79
15	45.3	45.0	30	24	6	0.80
16	47.1	47.5	32	26	6	0.81
18	51.5	51.3	36	28	8	0.78

Note. Basal spacing = line V in Fig. 3.

As shown in Table III, the length of the segments perpendicular to the layers (= *n_p*) increases with the total chain length (= *n_t*). With increasing chain length, the *gauche*-conformation is shifted to the free chain ends.

The segments inclined to the perpendicular cover *n_t - n_p* C-C bonds. This number is strikingly constant. For sufficient stability, the mean distance between the chains should not exceed 6 Å, which is the projection of an inclined segment with three C-C bonds to the layer (including the van der Waals thickness). For comparison: the highest chain packing density generally observed in *gauche*-blocks (33 Å²/chain) corresponds to a distance of 6.2 Å between the chains in a pseudo-hexagonal array. Thus, the chains in large-spacing structure form stable *gauche*-blocks with the *gauche*-bonds very near the free chain ends.

Intermediate Structure

If the interlayer chain density is decreased (for instance by vacuo-drying of the alkylamine intercalated silver molybdate), the length of the inclined segments increases to ensure a sufficient stability. This is realized by shifting the *gauche*-bond

away from the chain ends (Figs. 4b and c). Thus, *n_p/n_t* = 0.37 is markedly lower than for the long-spacing complexes (*n_p/n_t* = 0.6–0.8). The difference *n_t - n_p* is no more constant but increases with the total chain length (Table IV).

Short-Spacing Structure

The spacings of the alkylammonium-exchanged silver molybdate (washed and dried) follow lines I or II. Their absolute values and $\Delta d_L/\Delta n = 1.33$ and 1.46 exceed the highest values for monolayers of perpendicular chains. The bilayers are characterized by *n_p* ≈ 2 (*n* > 8). The chains in nearly full length are inclined to the layers, the arrangement resembles tilted bilayers with $\alpha = 35^\circ$ (Fig. 4d). A significant feature is the large end group distance on the molybdate layer and a high chain packing density between the tilted chains. With a cross section of 20–24 Å²/chain each chain requires an area of 35–42 Å² on the molybdate layer. In hexagonal arrays this corresponds

TABLE IV
INTERMEDIATE *Gauche*-BLOCK STRUCTURE OF
ALKYLAMINE AND ALKYLAMMONIUM SILVER
MOLYBDATES (LINE III)

<i>n</i>	<i>d_L</i> obs. (Å)	<i>d_L</i> , calc. (Å)	<i>n_t</i>	<i>n_p</i>	<i>n_t - n_p</i>	<i>n_p/n_t</i>
11	29.4 ^a	29.9	22	8	14	0.36
12	30.7 ^a	31.2	24	8	16	0.33
13	32.7 ^a	32.4	26	8	18	0.31
	33.2 ^b	33.7		10	16	0.38
14	34.7 ^a	34.9	28	10	18	0.36
	35.0 ^b	34.9		10	18	0.36
15	36.8 ^a	36.2	30	10	20	0.33
	37.0 ^b	37.5		12	18	0.40
16	38.2 ^a	38.7	32	12	20	0.38
	38.9 ^b	38.7		12	20	0.38
17	40.7 ^b	41.2	34	14	20	0.41
18	42.8 ^b	42.5	36	14	22	0.39

^a Alkylamine-intercalated silver molybdate, vacuo-dried.

^b Alkylammonium-exchanged silver molybdate in equilibrium with alkylammonium nitrate solution.

to chain end distances of 6.4–7 Å (cf. Fig. 5 in Lagaly and Weiss Ref. (6)). The unit cell (area in the a - c plane 84.5 Å²) can then incorporate 4.0–4.8 alkyl chains. As seen from Table I, the number of interlayer alkyl chains (= RNH₂ + RNH₃⁺) is considerably smaller (<2 chains/unit) for $n < 13$ and only increases for the longest chains to 4.2. The increase in (RNH₂ + RNH₃⁺) for $n > 13$ is not related to a corresponding increase of the basal spacings (lines I and II in Fig. 3). This directly leads to the conclusion that the shorter chains are aggregated to form isolated clusters. Figure 2 also makes it evident that the filling up between these clusters is caused by incorporation of alkylamine molecules and is not due to an increased degree of cation exchange. The driving force for the additional intercalation is the increased van der Waals interaction between the longer chains.

Conclusion

The lattice of silver molybdate can be expanded by reaction with alkylammonium cations and alkylamine molecules. Both compounds penetrate between the layers and aggregate to form distinct structures.

In nearly all crystal structures of long chain compounds the alkyl chains adopt the all-*trans* conformation and form quite close-packed units (about 19 Å²/chain). A general hypothesis that long chain compounds in layered host materials behave quite similarly, cannot be corroborated. The exchange of alkylammonium ions for interlayer cations generally leads to aggregations in which the alkyl chains adopt conformations with *gauche*-bonds (8). Alkylammonium-exchanged silver molybdate shows the variety of these structures. The chains are arranged in *gauche*-blocks because the interaction with the molybdate layer holds the polar chain ends (–NH₃⁺, –NH₂ groups) at relatively long distances

and renders impossible the close chain packing near the solid surface. The specially favored formation of *gauche*-blocks and their pronounced stability impede the quantitative cation exchange.

An exact determination of the chain arrangements by crystal structure determination actually cannot be performed because the crystals disintegrate to powders during the reaction. A further point is that the interlayer structure does not permit establishment of the high order and regularity required for crystal structure determinations. Thus, the interlayer structure must be deduced from basal spacing measurements. Certainly, this procedure involves some arbitrariness, but the general type of interlayer organization can be clearly established.

References

1. K. BENEKE AND G. LAGALY, *Z. Naturforsch.* **33b**, 564 (1978).
2. B. M. GATEHOUSE AND P. LEVERETT, *J. Chem. Soc. A* 1398 (1968).
3. B. M. GATEHOUSE AND P. LEVERETT, *Chem. Commun.* 1093 (1969).
4. B. M. GATEHOUSE AND P. LEVERETT, *J. Solid State Chem.* **1**, 484 (1970).
5. R. KOHLMÜLLER AND J. P. FAURIE, *Bull. Chem. Soc. Fr.* **11**, 4379 (1968).
6. G. LAGALY AND A. WEISS, *Kolloid Z. Z. Polym.* **238**, 485 (1970).
7. G. LAGALY, *Angew. Chem. Int. Ed. Engl.* **15**, 575 (1976).
8. G. LAGALY, *Naturwissenschaften* **68**, 82 (1981). (1981).
9. G. LAGALY, *Clay Miner.* **16**, 1 (1981).
10. F. LÉVY, (Ed.), "Intercalated Layered Materials," Reidel, Dordrecht/Boston/London (1979).
11. W. PECHHOLD, E. LISKA, H. P. GROSSMANN, AND P. C. HÄGELE, *J. Pure Appl. Chem.* **46**, 115 (1976).
12. J. E. RICCI AND W. F. LINKE, *J. Amer. Chem. Soc.* **73**, 3601 (1951).
13. A. WEISS, G. LAGALY, AND K. BENEKE, *Z. Pflanzenernaehr. Bodenkd.* **129**, 193 (1971).
14. M. ST. WHITTINGHAM AND A. J. JACOBSON, "Intercalation Chemistry," Academic Press, New York/London (1982).